Synthesis, QSAR and anticandidal evaluation of 1,2,3-triazoles derived from naturally bioactive scaffolds

ARTICLE *in* EUROPEAN JOURNAL OF MEDICINAL CHEMISTRY · FEBRUARY 2015

Impact Factor: 3.45 · DOI: 10.1016/j.ejmech.2015.02.007

European Journal of Medicinal Chemistry 93 (2015) 246–254

Contents lists available at ScienceDirect

European Journal of Medicinal Chemistry

journal homepage: http://www.elsevier.com/locate/ejmech

Preliminary communication

Synthesis, QSAR and anticandidal evaluation of 1,2,3-triazoles derived from naturally bioactive scaffolds

Mohammad Irfan [a, b], Babita Aneja [a], Umesh Yadava [c], Shabana I. Khan [d], Nikhat Manzoor [b], Constantin G. Daniliuc [e], Mohammad Abid [a, *]

[a] Medicinal Chemistry Lab, Department of Biosciences, Jamia Millia Islamia, New Delhi 110025, India
[b] Medical Mycology Lab, Department of Biosciences, Jamia Millia Islamia, New Delhi 110025, India
[c] Department of Physics, Deen Dayal Upadhyay Gorakhpur University, Gorakhpur, UP 273009, India
[d] National Center for Natural Products Research (NCNPR), School of Pharmacy, University of Mississippi, MS 38677, USA
[e] Organisch-Chemisches Institut, Westfalische Wilhelm-Universitat Munster, 48149, Germany

ARTICLE INFO

Article history:
Received 31 August 2014
Received in revised form
2 February 2015
Accepted 6 February 2015
Available online 7 February 2015

Keywords:
Candida
QSAR
Triazole
X-ray diffraction
Hemolysis
Cytotoxicity
Fluconazole

ABSTRACT

In the present study, we used eight natural precursors (**1a-h**) with most of them having promising antimicrobial activities and synthesised their novel 1,2,3-triazole derivatives **(3a-h**). In the reaction sequences, the precursor compounds **(1a-h)** were converted to their respective alkyne (**2a-h**) followed by addition of benzyl azide freshly prepared by the reaction of benzyl bromide with sodium azide using [3 + 2] azide-alkyne cycloaddition strategy. Structural elucidation of all the triazole derivatives was done using FT-IR, ^{1}H, ^{13}C NMR, mass and elemental analysis techniques. The single crystal X-ray diffraction for **3d** was also recorded. The result of *in vitro* anticandidal activity performed against three different strains of *Candida* showed that compound **3e** was found superior/comparable to fluconazole (**FLC**) with IC_{50} values of **0.044 μg/mL** against *Candida albicans* (ATCC 90028), **12.022 μg/mL** against *Candida glabrata* (ATCC 90030), and **3.60 μg/mL** against *Candida tropicalis* (ATCC 750). Moreover, at their IC_{50} values, compounds **3e** and **3h** showed <5% hemolysis which indicates the non-toxic behaviour of these inhibitors. Cytotoxicity assay was also performed on VERO cell line and all the derivatives were found non-toxic up to the concentration of **10.0 μg/mL**. The *in silico* technique of 3D-QSAR was applied to establish structure activity relationship of the synthesized compounds. The results reveal the molecular fragments that play an essential role in improving the anticandidal activity.

1. Introduction

Fungal infections pose a continuous and serious threat to human health. Among them, the incidents of *Candida* infection have increased substantially in recent years especially in immune-compromised patients and those with human immunodeficiency virus infections. According to a report of CDC 2013, *Candida* is the fourth most common cause of healthcare-associated bloodstream infections in the United States. It is estimated that approximately 30% of patients with bloodstream infections (*candidemia*) with drug-resistant *Candida* die during their hospitalization [1]. Antifungal drugs currently used for the treatment of *Candida* infections include polyenes, azoles, echinocandins, allyamines, and flucytosine. Among them, azole drugs have an important class of triazole antifungal agents like fluconazole, itraconazole, voriconazole and posaconazole (Fig. 1) which becomes the group of most widely used therapeutic antifungal agents with low toxicity, oral bioavailability, and broad spectrum [2]. However, the incidents of drug resistance, specially the front line antifungal drug fluconazole, have increased with a very rapid rate. Therefore, there is an urgent need to develop antifungal agents with novel structure and mode of action.

The triazole based compounds are well known for their wide range of biological activity such as antineoplastic [3], antimicrobial [4], analgesic [5], anti-inflammatory [6], local anesthetic [7], anticonvulsant [8], antimalarial [9] and anti-HIV agents [10]. Prompted by these observations and in continuation our efforts to develop structurally diverse organic scaffolds [11,12], we designed the synthesis of new series of 1,2,3-triazole derivatives from biologically active natural scaffolds (Fig. 2). The main reason for the

* Corresponding author.
E-mail address: mabid@jmi.ac.in (M. Abid).

http://dx.doi.org/10.1016/j.ejmech.2015.02.007
0223-5234/

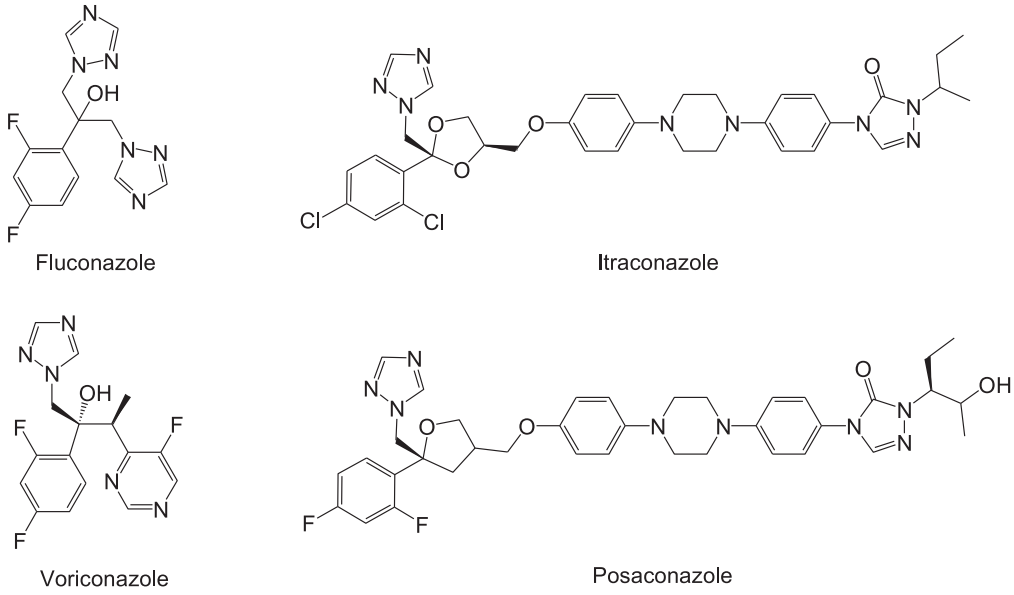

Fig. 1. Structure of azole based antifungal drugs.

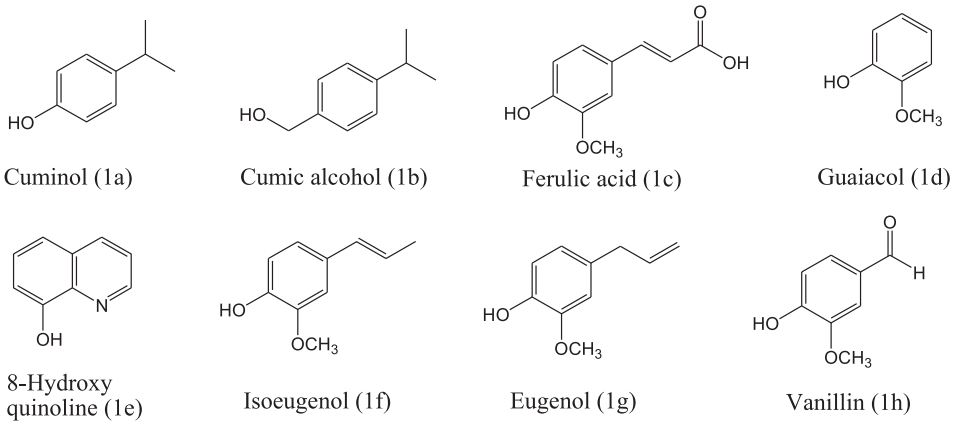

Fig. 2. Structure of precursor molecules (**1a-h**) used in the study.

synthesis was the diverse array of bioactivities possessed individually by them and to study the effect on the biological activity after their conversion into 1,2,3-triazole derivatives.

2. Results and discussion

2.1. Chemistry

A series of novel 1,2,3-triazole derivatives (**3a-h**) was synthesized as shown in Scheme 1. The precursor molecules (**1a-h**) were converted into 1,2,3-triazoles via copper catalyzed [3 + 2] azide-alkyne cycloaddition reaction. The hydroxyl group present in precursor compounds (**1a-h**) on treatment with propargyl bromide and K_2CO_3 in anhyd. DMF at 0 °C to room temperature gave the corresponding alkyne derivatives (**2a-h**). The reaction was completed in 18–24 h depending upon the structure of precursor molecule. In the other set of reaction, benzyl bromide was treated with sodium azide (NaN_3) in anhyd. DMF under reflux condition to give benzyl azide in excellent yield. Finally, azide-alkyne cycloaddition in ter. BuOH: H_2O (1:2) mixture and catalytic amount of copper sulphate and sodium ascorbate at room temperature for 48–72 h gave the title compounds (**3a-h**). The crude obtained was purified by silica gel chromatography using 10% methanol in dichloromethane as eluent to provide the title compounds **(3a-h)** in good to excellent yields. The proposed structures were confirmed by elemental analysis, FT IR, ^{1}H, ^{13}C NMR & Mass spectral data (Table 1). The single crystal X-ray diffraction for **3d** was also recorded.

2.1.1. IR analysis

In the IR spectra of all the compounds (**3a-h**), the main evidence for their formation came from the disappearance of absorption band at 2090 cm^{-1}corresponding to azido functionality indicating that azide had been completely consumed in the reaction and the peak corresponding to alkyne ≡C*H* and C≡C which appeared in the range 3250–3376 cm^{-1} and 2112–2137 cm^{-1} respectively was also absent from their spectra. All the synthesized compounds (**3a-h**) gave characteristic peak of triazole ring in the region 3065–3189 cm^{-1} as broad absorption bands. All the other absorption bands also appeared at the expected regions.

2.1.2. ^{1}H NMR analysis

In the ^{1}H NMR spectra, these compounds showed a sharp singlet in the region δ 7.18–7.67 ppm assigned to triazole ring, thus

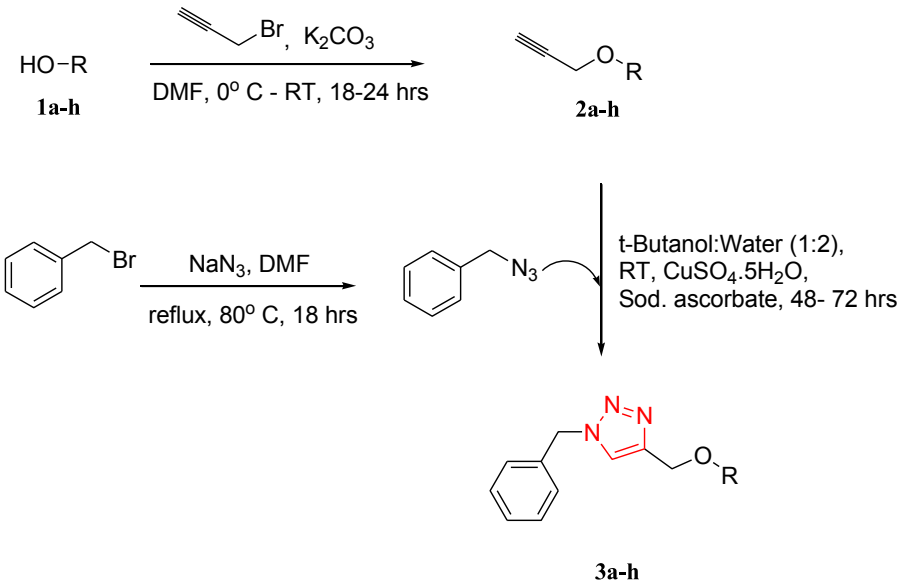

Scheme 1. General route of synthesis for triazole derivatives (**3a-h**).

confirming its formation. The characteristic singlets at δ 5.54–4.66 ppm and δ 5.50–4.36 ppm were also observed for OCH_2 and $C_6H_5CH_2$ protons of triazole derivatives **(3a-h)** respectively. While a sharp singlet corresponding to ≡*CH* group which appeared in the region δ 2.49–2.57 ppm was absent from the spectra. In addition, all the aromatic and aliphatic protons appeared at the expected chemical shifts and integral values.

2.1.3. ^{13}C NMR analysis

The cyclization of all alkynes with benzyl azide to triazole ring was further reconfirmed by ^{13}C NMR spectral data in which both the carbons of triazole ring appeared in the range δ 120.23–127.34 ppm and δ 138.32–145.92 ppm. The carbon signals of OCH_2 and $C_6H_5CH_2$ groups were resonated at δ 62.16–65.23 ppm and δ 54.25–55.99 ppm respectively, while all the other carbons gave peaks at their expected values.

2.1.4. Mass analysis

The mass spectra of all the compounds **(3a-h)** showed $[M+H]^+$ peak which is in accordance with the molecular formula of the compounds thus further reconfirming their formation. Some of the compounds showed $[2\ M + Na]^+$ peak in the mass spectra which suggests the dimerization of the molecular ion peak. In the mass spectra of compound **3b**, molecular ion peak was obtained with very low intensity and a fragment peak 133.2 corresponding to $[M\text{-}C_{10}H_{10}N_3O]^+$ was observed as the base peak.

2.2. X-ray crystallographic analysis

Crystal structure analysis of compound **3d** reveals that it crystallizes in monoclinic crystal system with space group $P2_1/c$. The data collection and structure refinement details are described in Table 2. 17347 reflections collected were collected out of which 2628 reflections were independent with $R_{int} = 0.041$. The number of observed reflections having $I > 2\sigma(I)$ was 2386. Finally, after refinement, a reasonably good R factor was found (R = 0.036). The hydrogen atom at C2 was refined freely but others were calculated and refined as riding atoms. The ORTEP diagram [13] of the compound **3d** with ellipsoids drawn at 50% probability level along with atomic numbering scheme is shown in Fig. 3. All the three aromatic rings N1–N2–N3–C2–C1, C11–C12–C13–C14–C15–C16 and C21–C122–C23–C24–C25–C26 are planar [maximum deviations of atoms from there least squares planes are 0.001(1)Å, 0.006(1)Å and 0.014(1)Å, respectively]. The planes containing aromatic rings C11–C16 and C21–C26 are inclined at an angle of 79.7(1)° while the ring N1–C1 form a bridge between them. The unit cell contains four molecules of similar conformations. In the crystal structure, the neighboring two molecules are arranged in anti-parallel manner in such a way that they form dimmer through intermolecular C–H … π interactions (Fig. 4). There are also weak intermolecular C–H···N hydrogen bonding interactions involving C4 and N1 atom at symmetry position −1 + X, Y, Z [d(H4B–N1) = 2.590, C4–H4B···N1 = 170.0].

2.3. Anticandidal evaluation

The inhibitory potential of synthesized 1,2,3-triazole derivatives (**3a-h**) was evaluated against three different strains of *Candida*: *C. albicans* ATCC 90028, *C. glabrata* ATCC 90030 and *Candida tropicalis* ATCC 750 and the results were compared with their precursors (**1a-h**) as well as standard drug fluconazole (**FLC**). The IC_{50} values in μg/mL and minimum fungicidal concentrations (MFC) were estimated and the results are summarized in Table 3. The objective of this study was to see the effect of structural transformation on the original anticandidal activity attributed to these natural precursors. The results showed that the original bioactivity of precursor molecules (**1a-h**) was lost except in case of **1e** and **1h** which showed many fold enhanced activity after structural transformation into triazoles i.e. **3e** and **3h**, respectively. Compounds **1a**, **1c**, and **1g** were found to be good inhibitors of *C. tropicalis* with IC_{50} values of 69.50 μg/mL, 67.60 μg/mL, and 92.68 μg/mL, respectively while their structural transformed **3a**, **3c**, and **3g** were found less active with IC_{50} values of 493.17 μg/mL, 105.12 μg/mL, and 734.00 μg/mL against same organism. Compounds **1b** showed very good anticandidal activity against *C. glabrata* with IC_{50} value of 7.09 μg/mL as compare to its triazole derivative **3b** which showed poor IC_{50} value of 316.15 μg/mL. Similarly, compounds **1d** and **1f** exhibited moderate anticandidal activity against all tested strains with IC_{50} value <350 μg/mL and <130 μg/mL, respectively but their structural derivatives **3d** and **3f** showed less effect on the growth of *Candida* spp.

Table 1
Structure of 1,2,3-triazole derivatives (**3a-h**).

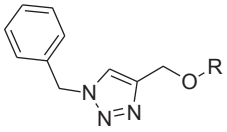

Compound	R	Structure of compound	Mol. formula	Reaction time
3a	1a	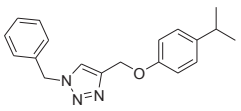	$C_{19}H_{21}N_3O$	18 h
3b	1b	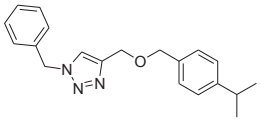	$C_{20}H_{23}N_3O$	72 h
3c	1c	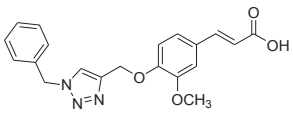	$C_{20}H_{19}N_3O_4$	40 h
3d	1d	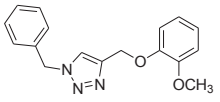	$C_{17}H_{17}N_3O_2$	50 h
3e	1e	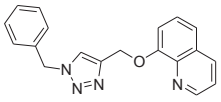	$C_{19}H_{16}N_4O$	69 h
3f	1f	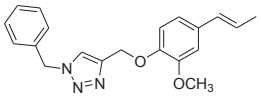	$C_{20}H_{21}N_3O_2$	64 h
3g	1g	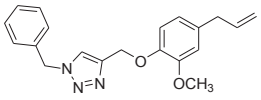	$C_{20}H_{21}N_3O_2$	18 h
3h	1h	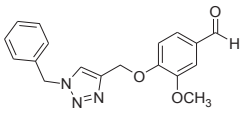	$C_{18}H_{17}N_3O_3$	64 h

Very interestingly, precursor compound **1e**, containing a quinoline ring with IC_{50} value of 13.80 μg/mL against *C. glabrata*, showed many fold increase in the anticandidal activity after its conversion into triazloe derivative **3e**. The derivative **3e** emerged as most potent inhibitor with IC_{50} values of 0.044 μg/mL against *C. albicans*, 12.02 μg/mL against *C. glabrata*, and 3.60 μg/mL against *C. tropicalis* and the results were superior/comparable to standard drug **FLC**. Another naturally bioactive precursor **1h** showed increased inhibitory activity after structural conversion into triazole derivative **3h**. Compound **3h** with free −CHO group and 1,2,3-triazole ring showed good to moderate activity with IC_{50} value of 44.67 μg/mL against *C. albicans*, 215.77 μg/mL against *C. glabrata*, and 92.68 μg/mL against *C. tropicalis*. The study suggested that anticandidal activity of precursors (**1a-h**) was mainly due to their free −OH group which is lost after conversion into 1,2,3 triazole derivatives (**3a-h**). The enhanced anticandidal activity of compounds **3e** and **3h** might be occurred due to presence of quinoline ring and free aldehyde group, respectively along with 1,2,3 triazole ring in their structures.

Table 2
Crystal data and structure refinement details for **3d**.

Identification code	**3d**
Empirical formula	$C_{17}H_{17}N_3O_2$
Formula weight	295.34
Temperature	223(2) K
Wavelength	0.71073 Å
Crystal system, space group	monoclinic, $P2_1/c$
Unit cell dimensions	a = 5.6192(1) Å, b = 15.4234(1) Å, c = 17.2628(1) Å, β = 94.236(1)°
Volume	1492.03(3) $Å^3$
Z, calculated density	4, 1.315 Mg/m^3
Absorption coefficient	0.715 mm^{-1}
F(000)	624
Crystal size	0.15 × 0.12 × 0.07 mm
Theta range for data collection	3.85–67.32°
Limiting indices	$0 \le h <= 6$, $0 \le k <= 18$, $-20 \le l <= 20$
Reflections collected/unique	17347/2628 [R(int) = 0.041]
Completeness to theta = 67.32	97.8%
Absorption correction	Semi-empirical from equivalents
Max. and min. transmission	0.9517 and 0.9003
Refinement method	Full-matrix least-squares on F^2
Data/restraints/parameters	2628/0/204
Goodness-of-fit on F^2	1.067
Final R indices [I > 2s(I)]	R1 = 0.0368, wR^2 = 0.0940
R indices (all data)	R1 = 0.0402, wR^2 = 0.0975
Largest diff. peak and hole	0.116 and −0.177 e.$Å^{-3}$

The MFC values favoured the fungistatic nature of precursor compounds (**1a-h**) and their 1,2,3-triazole derivatives (**3a-h**).

2.4. Synergistic studies

The *in vitro* synergistic anticandidal activity of most potent derivative **3e** in combination with **FLC** was determined for all the three strains of *Candida* (Table 4). The results showed that compound **3e** alone showed good inhibitory activities against all tested *Candida* species. The fractional inhibitory concentration index (FICI) values of compound **3e** were 0.74 for *C. albicans*, 0.48 for *C. glabrata* and 0.74 for *C. tropicalis*, respectively. The results of synergistic studies indicated that compound **3e** showed no synergistic activity in combination with FLC against *C. albicans* and *C. tropicalis* but showed moderate synergy against *C. glabrata*.

2.5. Cytotoxicity assays

2.5.1. Hemolysis

On the basis of *in vitro* anticandidal activity results, compounds **3e**, **3h** and their precursors (**1e** and **1h**) were selected to check their cytotoxic effect on human red blood cells (hRBCs) by hemolytic assay. The toxicity of standard drug fluconazole was also determined for reference. At the concentration of 500 μg/mL, compounds **1e**, **1h**, **3e** and **3h** showed 14.97, 5.45, 4.76 and 33.5% hemolysis while standard drug fluconazole showed 68.63% hemolysis (Fig. 5). At their IC_{50} values, compounds **1e**, **1h**, **3e** and **3h** showed <5% hemolysis which indicates that these compounds have very low or no cytotoxic effect on human RBCs.

2.5.2. Cytotoxicity by cell proliferation assay

To examine the toxicity of all triazole derivatives (**3a-h**) on cell proliferation, they were screened for cytotoxicity against monkey kidney fibroblasts (VERO) and the results are shown in Table 3. A subconfluent population of VERO cells was treated with increasing concentration of active compounds and the number of viable cells was measured after 48 h by MTT cell viable assay. The IC_{50} values were calculated and Doxorubicin was used as control. None of the compound was found cytotoxic upto the concentration of **10 μg/mL**.

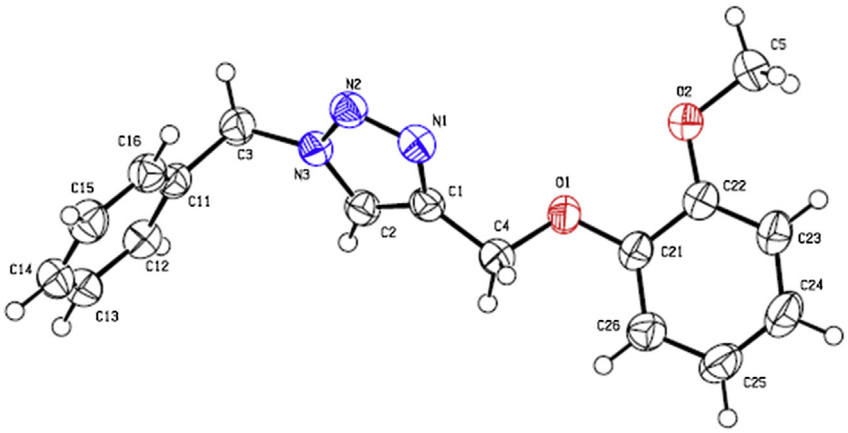

Fig. 3. ORTEP diagram of compound **3d** with atomic labeling scheme (Displacement ellipsoids are drawn at 50% probability level).

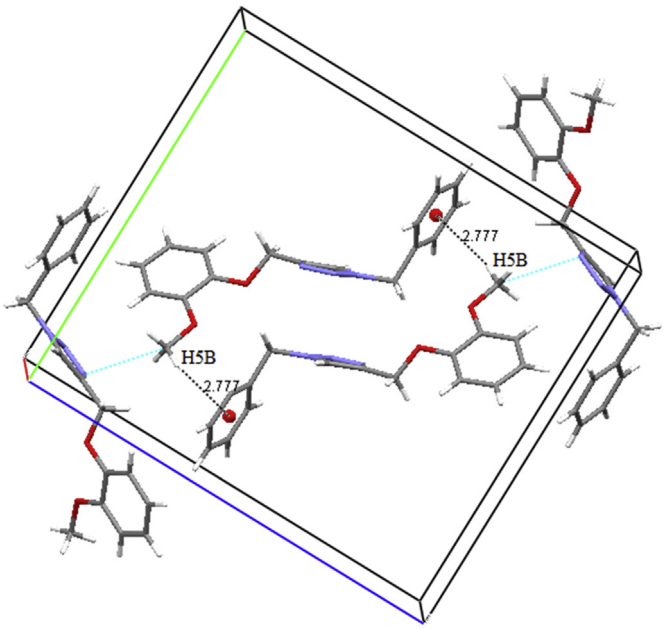

Fig. 4. Unit cell diagram in the crystal packing of compound **3d** showing intermolecular C—H … π hydrogen bonding.

2.6. QSAR studies

The data set of 16 compounds was divided randomly into training set of 12 compounds and test set of 4 compounds (75 and 25% respectively of the total number of compounds). When these compounds were subjected to QSAR analysis, in order to develop QSAR models, various statistically significant two parametric models were obtained. For each type of descriptors, the best multilinear regression equations were obtained by the stepwise selection methods of Heuristic subroutine of the software. The squared correlation coefficient (R^2), standard error of estimate (r^2_se) and Fisher's value (F) which represents the F-ratio between the variance of actual and predicted activity, were employed to judge the validity of the model. The results of regression models are shown.

2.6.1. QSAR model 1

In the first model, QSAR study was carried out on the activities of a series of substituted triazole derivatives for *C. albicans* inhibitors. Compounds **1b**, **1c**, **3b** and **3c** were chosen for test set while others for training set. Among 163 descriptors, that were considered in generating the QSAR model, few descriptors such as partial positive surface area, partial negative surface area, total molecular surface area, XY or YZ shadow, average information content, total number of 'O' or 'N' atoms, number of aromatic rings etc. play important roles in developing the QSAR model. Five descriptors were used to develop the QSAR model. The calculated statistical parameters ($R^2 = 0.995$ and $F = 255.179$) based on the Heuristic method, were found to be quite good to be considered as the best QSAR model. In addition, the randomization test is also good indicating the better model. Also, for the validation of the QSAR model, we went through the test set via the training set. The results obtained for the test set is $R^2_{test} = 0.999$, $F_{test} = 3692.1509$. RMSEs are found to be 0.5 and 0.6% respectively for training and test sets respectively. The squared correlation coefficient for the test set and training set near '1' and very small values of RMSEs prove the validity of the generated QSAR model.

2.6.2. QSAR model 2

In the second QSAR model the compounds which were chosen for test set are **1b**, **1h**, **3e** and **3h**. Other compounds were used as the training set. QSAR model developed using heuristic method, based on the inhibition activities of triazole derivatives against *C. glabrata* indicate that the squared cross correlation factor and Fischer values are 0.958 and 27.327 for training set of 12 compounds while 0.997 and 1868.48 for test set of 4 compounds. A total of 163 descriptors were calculated which include geometrical, constitutional, topological, electrostatic, quantum mechanical and thermodynamic descriptors. The five descriptors which play important role in developing QSAR model are minimum partial charge for C-atom, weighted partial positive surface area, number of 'O' atoms, average information content and HACA-1. RMSEs as obtained through calculations are found to be 8.6% and 0.9% respectively. The validation test on the model clearly demonstrate that the developed model represent the valid model in which electrostatic descriptors play important roles.

2.6.3. QSAR model 3

On the basis of experimental activities of compounds for the inhibition of *C. tropicalis*, QSAR model is developed using Heuristic method. Four compounds chosen for test set are **1e**, **1c**, **3f** and **3g** while rests were used for training set. Developed QSAR model on training set show that the cross correlation factor and Fischer values are reasonably good ($R^2 = 0.923$, $F = 31.793$). Among 163 calculated descriptors, five descriptors namely; fractional HDSA-1,

Table 3
Anticandidal evaluation of 1,2,3-triazoles and their precursor molecules.

Compound	Anticandidal properties						Cytotoxicity
	C. albicans ATCC 90028		*C. glabrata* ATCC 90030		*C. tropicalis* ATCC 750		VERO
	IC_{50} ± S.D. (μg/mL)	MFC (μg/mL)	IC_{50} ± S.D. (μg/mL)	MFC (μg/mL)	IC_{50} ± S.D. (μg/mL)	MFC (μg/mL)	IC_{50} (μg/mL)
1a	181.55 ± 0.33	500	153.46 ± 0.76	>1000	69.50 ± 0.56	>1000	ND
1b	81.47 ± 1.10	1000	7.09 ± 0.64	500	44.77 ± 0.08	1000	ND
1c	210.37 ± 0.69	>1000	616.59 ± 0.55	>1000	67.60 ± 0.78	>1000	ND
1d	179.06 ± 0.18	>1000	335.73 ± 0.92	>1000	201.37 ± 1.02	>1000	ND
1e	18.47 ± 0.06	500	13.80 ± 0.70	500	22.90 ± 0.91	500	ND
1f	82.98 ± 0.89	1000	71.61 ± 0.66	500	127.73 ± 0.73	1000	ND
1g	236.59 ± 1.18	>1000	215.77 ± 0.81	>1000	92.68 ± 0.59	>1000	ND
1h	321.36 ± 0.60	>1000	483.06 ± 1.21	>1000	123.40 ± 0.79	>1000	ND
3a	549.67 ± 1.34	1000	1063.8 ± 1.74	1000	493.17 ± 0.87	1000	NA
3b	324.49 ± 0.46	>1000	316.15 ± 0.94	>1000	169.43 ± 0.83	>1000	NA
3c	891.25 ± 0.68	>1000	416.48 ± 0.57	>1000	105.12 ± 0.07	>1000	NA
3d	514.63 ± 0.94	ND	369.83 ± 0.94	>1000	165.12 ± 0.70	ND	NA
3e	0.044 ± 0.11	62.5	12.02 ± 0.02	125	3.60 ± 0.07	62.5	NA
3f	480.83 ± 1.23	ND	292.76 ± 0.93	>1000	154.00 ± 0.85	>1000	NA
3g	1094.4 ± 1.87	>1000	847.23 ± 1.32	>1000	734.00 ± 1.37	ND	NA
3h	44.67 ± 0.76	>500	215.77 ± 1.41	500	92.68 ± 0.83	500	NA
FLC	15.62 ± 0.65	ND	7.81 ± 0.88	ND	8.55 ± 1.59	ND	ND
D	ND	ND	ND	ND	ND	ND	>5

FLC = Fluconazole, D = Doxorubicin, NA = no activity upto 10 μg/mL, ND = not done.

Table 4
In vitro Synergistic anticandidal activity of compound **3e**.

Organism	MIC alone		MIC in combination		FICI[a]	Mode of interaction
	3e	**FLC**	**3e**	**FLC**		
C. albicans ATCC 90028	15.62	31.25	7.81	7.81	0.74	Indifferent
C. glabrata ATCC 90030	31.25	15.62	7.81	3.90	0.48	Synergy
C. tropicalis ATCC 750	15.62	15.62	7.81	3.90	0.74	indifferent

[a] Synergy and antagonism were defined by FICI ≤0.5 and >4, respectively. Indifferent was defined by 0.5 < FICI ≤4.

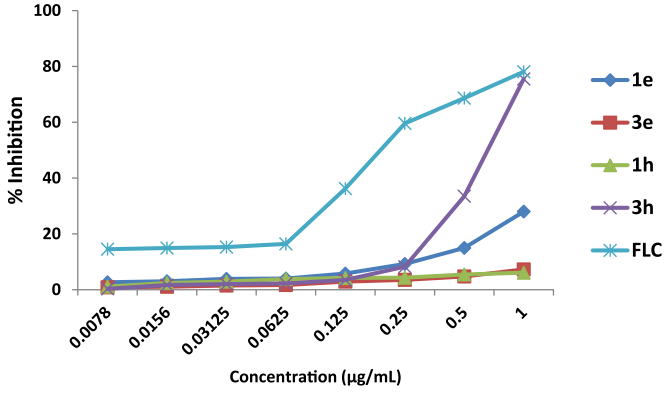

Fig. 5. Hemolysis activity of compounds of **1e**, **1h**, **3e**, **3h** and FLC.

fractional PPSA, relative number of rings, number of 'O' atoms and HDCA-1 were used for developing the model. To validate the model, we went through the test set via training set. The results obtained are R2test = 0.835, Ftest = 10.133. The validation tests on the model demonstrate 13.8 and 19.1% root mean square error for training and test sets respectively.

3. Conclusion

In summary, a novel series bearing 1,2,3-triazole ring (**3a-h**) was designed and synthesized as potent inhibitors of *candida* species. Compound **3e** and **3h** showed many fold increase in the anticandidal activity in comparison to their precursors and were also found non-toxic by hemolytic assay as well on cell proliferation assay on VERO cells. QSAR models were developed using Heuristic method on the studied compounds. The FICI results indicated that there is no synergistic activity in compound **3e** in combination with FLC against *C. albicans* and *C. tropicalis* but showed moderate synergy against *C. glabrata*. Further structural optimization, *in vivo* studies and their mode of action may lead to the development of these prototype molecules into potential antifungal agents.

4. Experimental section

4.1. Chemistry

All the reagents and solvents purchased from Sigma-Aldrich, S.D. Fine, SRL and Hi Media, were used without further purification. Reaction was monitored by thin-layer chromatography (TLC) using pre coated aluminium sheets (Silica gel 60 F_{254}, Merck Germany) and spots were visualized under UV light. The IR spectra of the compounds were recorded on Agilent Cary 630 FT-IR spectrometer. ^{1}H NMR and ^{13}C NMR spectra were obtained in $CDCl_3$with reference to TMS as internal standard using Bruker Spectrospin DPX-300 spectrometer at 300 MHz and 75 MHz respectively. Splitting patterns are designated as follows: s, singlet; d, doublet; t, triplet; m, multiplet. Chemical shift (δ) values are given in parts per million (ppm) and coupling constants (J) in Hertz (Hz). Mass spectra were carried out on Agilent LC- 1200 series MS/MS-6410 spectrometer. CHN analysis was recorded on Elemental Vario analyzer. Melting points were recorded on a digital Buchi melting point apparatus (M–560) and were reported uncorrected. Purification of the compounds was done by column chromatography using silica gel (230–400 mesh size) with Petroleum Ether/Ethyl acetate (8:2) as eluent for alkynes and 10% methanol in DCM for triazole derivatives.

4.1.1. General procedure for the synthesis of alkynes (***2a-h***)

A round bottom flask with stir bar was charged with natural precursor (1eq) and anhyd. DMF (10 mL) and the reaction flask was cooled to 0 °C. To this solution, potassium carbonate (1eq) was added, followed by slow addition of propargyl bromide (1.2 eq). The

reaction mixture was allowed to warm to room temperature and stirred overnight under argon. After completion of the reaction as confirmed by TLC, it was concentrated and water was added to the residue. The compound was extracted with ethyl acetate, dried over anhydrous sodium sulphate and concentrated under vacuum. The crude was purified by column chromatography using 20% ethyl acetate in petroleum ether to give the desired alkynes (**2a-h**) in good to excellent yields [14].

*4.1.1.1. 1-Isopropyl-4-(prop-2-ynyloxy)benzene (**2a**).* Pale yellow oil, yield: 92%, R_f (Ethyl acetate/Pet. ether, 20:80) = 0.54, Anal ($C_{12}H_{14}O$) calc. C 82.72 H 8.10, found: C 82.69 H 8.08%. IR (neat): ν (cm^{-1}) 3293, 2981, 2872, 1613, 1587, 1512, 1460, 1330, 1290, 1264, 1218, 1182, 1030, 990, 830, 672. ^{1}H NMR (300 MHz, $CDCl_3$) (δ, ppm): 7.19 (d, 2H, *J* = 8.1 Hz, Ar−*H*), 6.94 (d, 2H, *J* = 8.1 Hz, Ar−*H*), 4.67 (s, 2H, OCH_2), 2.94−2.88 (m, 1H, C*H*), 2.54 (s, 1H, ≡C*H*), 1.26 (d, 6H, *J* = 6.9 Hz, CH_3).

*4.1.1.2. 1-Isopropyl-4-((prop-2-ynyloxy)methyl)benzene (**2b**).* Pale yellow oil, yield: 73%, R_f (Ethyl acetate/Pet. ether, 20:80) = 0.65, Anal ($C_{13}H_{16}O$) calc. C 82.94 H 8.57, found: C 82.91 H 8.55%. IR (neat): ν (cm^{-1}) 3339, 2981, 2931, 2131, 1672, 1524, 1475, 1418, 1387, 1359, 1254, 1212, 1062, 1021, 854, 815, 745, 710. ^{1}H NMR (300 MHz, $CDCl_3$) (δ, ppm): 7.43 (d, 2H, *J* = 8.7 Hz, Ar−*H*), 7.31 (d, 2H, *J* = 8.7 Hz, Ar−*H*),4.61 (s, 2H, OCH_2), 4.32 (s, 2H, OCH_2), 2.92−2.89 (m, 1H, C*H*), 2.52 (s, 1H, ≡C*H*), 1.23 (d, 6H, *J* = 7.9 Hz, CH_3).

*4.1.1.3. (E)-3-(3-methoxy-4-(prop-2-ynyloxy)phenyl)acrylic acid (**2c**).* Off-white solid, yield: 98%, R_f (Ethyl acetate/Pet. ether, 50:50) = 0.54, Anal ($C_{13}H_{12}O_4$) calc. C 67.23 H 5.21, found: C 67.20 H 5.19%. IR (neat): ν (cm^{-1}) 3376, 3298, 2959, 2926, 2855, 2125, 1710, 1623, 1596, 1511, 1487, 1413, 1310, 1257, 1143, 1023, 954, 724. ^{1}H NMR (300 MHz, $CDCl_3$) (δ, ppm): 7.68 (d, 1H, *J* = 15.9 Hz, =C*H*), 7.06−7.02 (m, 2H, Ar−*H*), 6.92 (d, 1H, *J* = 8.1 Hz, Ar−*H*), 6.31 (d, 1H, *J* = 15.9 Hz, =C*H*), 4.81 (s, 2H, OCH_2), 3.92 (s, 3H, OCH_3), 2.55 (s, 1H, ≡C*H*).

*4.1.1.4. 1-Methoxy-2-(prop-2-ynyloxy)benzene (**2d**).* Yellow oil, yield: 98%, R_f (Ethyl acetate/Pet. ether, 20:80) = 0.62, Anal ($C_{10}H_{10}O_2$) calc. C 74.06 H 6.21, found: C 74.03 H 6.18%. IR (neat): ν (cm^{-1}) 3286, 3070, 2936, 2840, 2125, 1674, 1596, 1503, 1462, 1376, 1331, 1253, 1212, 1182, 1127, 1026, 929, 847, 743. ^{1}H NMR (300 MHz, $CDCl_3$) (δ, ppm): 7.35−7.32 (m, 2H, Ar−*H*), 7.24−7.21 (m, 2H, Ar−*H*), 4.92 (s, 2H, OCH_2), 3.87 (s, 3H, OCH_3), 2.52 (s, 1H, ≡C*H*).

*4.1.1.5. 8-(Prop-2-ynyloxy)quinoline (**2e**).* Dark brown solid, yield: 66%, R_f (Ethyl acetate/Pet. ether, 20:80) = 0.21, Anal ($C_{12}H_9NO$) calc. C 78.67 H 4.95 N 7.65, found: C 78.65 H 4.93 N 7.62%. IR (neat): ν (cm^{-1}) 3319, 2925, 2854, 2112, 1855, 1573, 1503, 1473, 1410, 1369, 1316, 1264, 1182, 1104, 1019, 996, 825, 795, 754, 728, 713, 665. ^{1}H NMR (300 MHz, $CDCl_3$) (δ, ppm): 8.82 (d, 1H, *J* = 8.7 Hz, Ar−*H*), 8.12 (d, 1H, *J* = 7.5 Hz, Ar−*H*), 7.56−7.47 (m, 3H, Ar−*H*), 7.32 (d, 1H, *J* = 8.1 Hz, Ar−*H*), 5.41 (s, 2H, OCH_2), 2.56 (s, 1H, ≡C*H*).

*4.1.1.6. (E)-2-methoxy-4-(prop-1-enyl)-1-(prop-2-ynyloxy)benzene (**2f**).* Off-white solid, yield: 98%, R_f (Ethyl acetate/Pet. ether, 20:80) = 0.68, Anal ($C_{13}H_{14}O_2$) calc. C 77.20 H 6.98, found: C 77.18 H 6.97%. IR (neat): ν (cm^{-1}) 3285, 3019, 2916, 2937, 2121, 1674, 1587, 1510, 1452, 1415, 1378, 1300, 1257, 1218, 1140, 1024, 964, 924, 910, 786 .^{1}H NMR (300 MHz, $CDCl_3$) (δ, ppm): 6.96−6.86 (m, 3H, Ar−*H*), 6.36 (d, 1H, *J* = 15.6 Hz, =C*H*), 6.17−6.10 (m, 1H, =C*H*), 4.76 (s, 2H, OCH_2), 3.89 (s, 3H, OCH_3), 2.51 (s, 1H, ≡C*H*), 1.88 (d, 3H, *J* = 6.6 Hz, CH_3).

*4.1.1.7. 4-Allyl-2-methoxy-1-(prop-2-ynyloxy)benzene (**2g**).* Yellow oil, yield: 79%, R_f (Ethyl acetate/Pet. ether, 20:80) = 0.56, Anal ($C_{13}H_{14}O_2$) calc. C 77.20 H 6.98, found: C 77.18 H 6.96%. IR (neat): ν (cm^{-1}) 3313, 2920, 2851, 2125, 1656, 1560, 1510, 1486, 1378, 1266, 1235, 1143, 1125, 1033, 996, 912, 799, 722. ^{1}H NMR (300 MHz, $CDCl_3$) (δ, ppm): 6.96 (d, 1H, *J* = 8.7 Hz, Ar−*H*), 6.73- 6.67 (m, 2H, Ar−*H*), 6.00−5.89 (m, 1H, =C*H*), 5.11−5.05 (m, 2H, =CH_2), 4.73 (s, 2H, OCH_2), 3.86 (s, 3H, OCH_3), 3.34 (d, 2H, *J* = 6.6 Hz, CH_2), 2.49 (s, 1H, ≡C*H*).

*4.1.1.8. 3-Methoxy-4-(prop-2-ynyloxy)benzaldehyde (**2h**).* Off white solid, yield: 98%,R_f (Ethyl acetate/Pet. ether, 20:80) = 0.54, Anal ($C_{11}H_{10}O_3$) calc. C 69.46 H 5.30, found: C 69.43 H 5.27%. IR (neat): ν (cm^{-1}) 3250, 2987, 2926, 2859, 2738, 2116, 1693, 1592, 1510, 1456, 1382, 1337, 1272, 1223, 1127, 1036, 1013, 927, 860, 814, 782, 720, 694. ^{1}H NMR (300 MHz, $CDCl_3$) (δ, ppm): 9.92 (s, 1H, C*H*O), 7.49−7.44 (m, 2H, Ar−*H*), 7.15 (d, 1H, *J* = 8.1 Hz, Ar−*H*), 4.87 (s, 2H, CH_2), 3.95 (s, 3H, OCH_3), 2.57 (s, 1H, ≡C*H*).

4.1.2. Procedure for the synthesis of benzyl azide

A mixture of benzyl bromide (1 eq) and sodium azide (3 eq) in anhyd. DMF (10 mL) was stirred overnight at 70 °C. After completion of the reaction as monitored by TLC, the reaction was quenched with water. The crude was extracted with ethyl acetate, washed with brine, dried over anhydrous sodium sulphate and concentrated under *vacuum*. The oily residue was used as such without any further purification [15].

*4.1.3. General procedure for the synthesis of triazole derivatives (**3a-h**)*

Equimolar amounts of alkyne (**2a-h**) and benzyl azide were dissolved in ter-butanol and water (1:2) mixture. To this reaction mixture, copper sulphate (0.05 eq) and sodium ascorbate (0.01 eq) were added and stirred at room temperature till the disappearance of starting materials as indicated by TLC. The reaction was quenched with saturated brine and crude was extracted with ethyl acetate, dried over anhydrous Na_2SO_4 and concentrated under vacuum. The crude was purified by column chromatography using 10% methanol in DCM as eluent to give 1,2,3-triazole derivatives in good to excellent yields [16].

*4.1.3.1. 1-Benzyl-4-((4-isopropylphenoxy)methyl)-1H-1,2,3-triazole (**3a**).* White solid, M.pt. 90−92 °C, yield: 90%, R_f (Ethyl acetate/Pet. ether, 30:70) = 0.48, Anal ($C_{19}H_{21}N_3O$) calc. C 74.24 H 6.89 N 13.67, found: C 74.20 H 6.85 N 13.64%. IR (neat): ν (cm^{-1}) 3126, 3070, 3041, 2962, 2869, 1614, 1588, 1514, 1462, 1383, 1365, 1305, 1287, 1249, 1220, 1182, 1134, 1115, 1063, 1030, 1007, 851, 832, 769, 702, 680. ^{1}H NMR (300 MHz, $CDCl_3$) (δ, ppm): 7.59 (s, 1H, triazole ring), 7.38−7.36 (m, 3H, Ar−*H*), 7.28−7.26 (m, 2H, Ar−*H*), 7.13 (d, 2H, *J* = 8.1 Hz, Ar−*H*), 6.89 (d, 2H, *J* = 8.4 Hz, Ar−*H*), 5.53 (s, 2H, OCH_2), 5.16 (s, 2H, CH_2), 2.90−2.81 (m, 1H, C*H*), 1.21 (d, 6H, *J* = 6.9 Hz, CH_3). ^{13}C NMR (75 MHz, $CDCl_3$) (δ, ppm): 156.29, 141.71, 134.45, 129.15, 128.84, 128.16, 127.34, 114.60, 62.16, 54.43, 33.27, 24.19. LC-MS (*m*/*z*): 308.3[M+H] $^+$, 637.4 [2 M + Na]$^+$.

*4.1.3.2. 4-((4-Isopropylbenzyloxy)methyl)-1-benzyl-1H-1,2,3-triazole (**3b**).* Yellow oil, yield: 76%, R_f (Ethyl acetate/Pet. ether, 30:70) = 0.61, Anal ($C_{20}H_{23}N_3O$) calc. C 74.74 H 7.21 N 13.07, found: C 74.71 H 7.19 N 13.05%. IR (neat): ν (cm^{-1}) 3189, 2961, 2929, 2872, 1516, 1460, 1423, 1385, 1365, 1257, 1207, 1059, 1017, 843, 817, 752, 700. ^{1}H NMR (300 MHz, $CDCl_3$) (δ, ppm): 7.57 (s, 1H, triazole ring), 7.43−7.24 (m, 9H, Ar−*H*), 4.66 (s, 4H, OCH_2), 4.36 (s, 2H, CH_2), 2.99−2.90 (m, 1H, C*H*), 1.28 (d, 6H, *J* = 6.9 Hz, CH_3). ^{13}C NMR (75 MHz, $CDCl_3$) (δ, ppm): 148.48, 138.32, 135.38, 128.88, 128.35, 128.26, 127.24, 126.66, 65.23, 54.82, 33.90, 29.74, 24.05. LC-MS (*m*/*z*): 322.2[M+H]$^+$,133.2 [M-$C_{10}H_{10}N_3O$]$^+$.

*4.1.3.3. (E)-3-(4-((1-benzyl-1H-1,2,3-triazol-4-yl)methoxy)-3-methoxyphenyl)acrylic acid (**3c**).* Off-white solid, M.pt. 83–85 °C, yield: 90%, R_f (Ethyl acetate/Pet. ether, 30:70) = 0.25, Anal ($C_{20}H_{19}N_3O_4$) calc. C 65.74 H 5.24 N 11.50, found: C 65.72 H 5.22 N 11.53%. IR (neat): ν (cm^{-1}) 3093, 3037, 2925, 2854, 1734, 1707, 1637, 1599, 1514, 1458, 1428, 1313, 1264, 1145, 1056, 1007, 989, 814, 724, 702, 668. ^{1}H NMR (300 MHz, $CDCl_3$) (δ, ppm): 7.63 (s, 1H, triazole ring), 7.59 (d, 1H, *J* = 5.7 Hz, =C*H*), 7.36–7.27 (m, 5H, Ar–*H*), 7.03 (d, 2H, *J* = 11.4 Hz, Ar–*H*), 6.90 (d, 1H, *J* = 8.1 Hz, Ar–*H*), 6.30 (d, 1H, *J* = 10.8 Hz, =C*H*), 5.52 (s, 2H, OCH_2), 5.31 (s, 2H, CH_2), 3.83 (s, 3H, OCH_3). ^{13}C NMR (75 MHz, $CDCl_3$) (δ, ppm): 166.97, 149.79, 148.28, 146.89, 145.28, 134.40, 129.16, 128.84, 128.17, 126.74, 123.65, 122.52, 115.53, 113.72, 110.17, 63.04, 55.88, 54.26. LC-MS (*m*/*z*):366.2 $[M+H]^+$.

*4.1.3.4. 1-Benzyl-4-((2-methoxyphenoxy)methyl)-1H-1,2,3-triazole (**3d**).* Brown crystalline solid, M.pt. 119–121 °C, yield: 78%, R_f (Ethyl acetate/Pet. ether, 30:70) = 0.18, Anal ($C_{17}H_{17}N_3O_2$) calc. C 69.14 H 5.80 N 14.23, found: C 69.11 H 5.77 N 14.21%. IR (neat): ν (cm^{-1}) 3131, 2972, 2931, 2877, 2834, 1685, 1588, 1497, 1452, 1434, 1389, 1313, 1251, 1216, 1181, 1121, 1059, 1028, 998, 918, 860, 808, 745, 672. ^{1}H NMR (300 MHz, $CDCl_3$) (δ, ppm): 7.57 (s, 1H, triazole ring), 7.38–7.36 (m, 3H, Ar–*H*), 7.28–7.26 (m, 2H, Ar–*H*), 7.05 (d, 1H, *J* = 7.5 Hz, Ar–*H*), 6.92 (d, 1H, *J* = 8.1 Hz, Ar–*H*), 6.89–6.86 (m, 2H, Ar–*H*), 5.52 (s, 2H, OCH_2), 5.28 (s, 2H, CH_2), 3.84 (s, 3H, OCH_3). ^{13}C NMR (75 MHz, $CDCl_3$) (δ, ppm): 149.67, 147.62, 144.74, 134.51, 129.10, 128.75, 128.13, 122.88, 121.94, 120.89, 114.60, 111.87, 63.33, 55.81, 54.17. LC-MS (*m*/*z*):296.3 $[M+H]^+$, 613.3 [2 M + Na]$^+$.

*4.1.3.5. 8-((1-Benzyl-1H-1,2,3-triazol-4-yl)methoxy)quinoline (**3e**).* Dark brown solid, M.pt. 82–84 °C, yield: 90%, R_f (Ethyl acetate/Pet. ether, 30:70) = 0.22, Anal ($C_{19}H_{16}N_4O$) calc. C 72.13 H 5.10 N 17.71, found: C 72.11 H 5.06 N 17.68%. IR (neat): ν (cm^{-1}) 3183, 3062, 1572, 1501, 1473, 1428, 1369, 1315, 1182, 1102, 994, 927, 823, 791, 750,709, 672. ^{1}H NMR (400 MHz, $CDCl_3$) (δ, ppm): 8.91 (d, 1H, *J* = 2.52 Hz, Ar–*H*), 8.13 (d, 1H, *J* = 8.32 Hz, Ar–*H*), 7.67 (s, 1H, triazole ring), 7.46–7.39 (m, 3H, Ar–*H*), 7.35–7.33 (m, 4H, Ar–*H*), 7.26–7.24 (m, 2H, Ar–*H*), 5.54 (s, 2H, OCH_2), 5.50 (s, 2H, CH_2). ^{13}C NMR (75 MHz, $CDCl_3$) (δ, ppm): 153.81, 149.30, 144.43, 140.19, 136.08, 134.34, 129.48, 128.78, 128.17, 126.49, 123.27, 121.93, 121.02, 120.23, 109.45, 62.96, 54.25. LC-MS (*m*/*z*): 317.2$[M+H]^+$, 655.3 [2 M + Na]$^+$.

*4.1.3.6. (E)-1-benzyl-4-((2-methoxy-4-(prop-1-enyl)phenoxy)methyl)-1H-1,2,3-triazole (**3f**).* Off-white solid, M.pt. 100–102 °C, yield: 75%, R_f (Ethyl acetate/Pet. ether, 30:70) = 0.28, Anal ($C_{20}H_{21}N_3O_2$) calc. C 71.62 H 6.31 N 12.53, found: C 71.59 H 6.28 N 12.51%. IR (neat): ν (cm^{-1})3065, 2924, 2851, 1721, 1605, 1587, 1512, 1460, 1423, 1380, 1343, 1296, 1262, 1225, 1162, 1140, 1061, 1035, 1018, 964, 855, 836, 737, 717, 678. ^{1}H NMR (300 MHz, $CDCl_3$) (δ, ppm): 7.54 (s, 1H, triazole ring), 7.37–7.35 (m, 3H, Ar–*H*), 7.26–7.24 (m, 2H, Ar–*H*), 6.95–6.80 (m, 3H, Ar–*H*), 6.32 (d, 1H, *J* = 15.9 Hz, =C*H*), 6.12–6.07 (m, 1H, =C*H*), 5.51 (s, 2H, OCH_2), 5.25 (s, 2H, CH_2), 3.84 (s, 3H, OCH_3), 1.89 (d, 3H, *J* = 6.3 Hz, CH_3). ^{13}C NMR (75 MHz, $CDCl_3$) (δ, ppm): 149.57, 146.62, 144.75, 134.44, 132.17, 130.50, 129.12, 128.78, 128.16, 124.31, 122.86, 118.62, 114.41, 108.94, 63.38, 55.78, 54.22, 18.41. LC-MS (*m*/*z*):336.3 $[M+H]^+$, 693.4 [2M + Na]$^+$.

*4.1.3.7. 4-((4-Allyl-2-methoxyphenoxy)methyl)-1-benzyl-1H-1,2,3-triazole (**3g**).* Pinkish white solid, M.pt. 78–80 °C, yield: 90%, R_f (Ethyl acetate/Pet. ether, 30:70) = 0.29, Anal ($C_{20}H_{21}N_3O_2$) calc. C 71.62 H 6.31 N 12.53, found: C 71.59 H 6.28 N 12.50%. IR (neat): ν (cm^{-1}) 3131, 3037, 3090, 2959, 2931, 2915, 2831, 1639, 1592, 1514, 1462, 1445, 1385, 1287, 1262, 1231, 1145, 1041, 1018, 924, 853, 836, 812, 717, 700. ^{1}H NMR (300 MHz, $CDCl_3$) (δ, ppm): 7.18 (s, 1H, triazole ring), 6.90 (d, 1H, *J* = 8.7 Hz, Ar–*H*), 6.77 (d, 1H, *J* = 8.7 Hz, Ar–*H*), 6.67- 6.62 (m, 4H, Ar–*H*), 5.92- 5.83 (m, 3H, Ar–*H*, =C*H*), 5.40 (s, 2H, OCH_2), 5.04–4.97 (m, 2H, =CH_2), 4.66 (s, 2H, CH_2), 3.80 (s, 3H, OCH_3), 3.27 (t, 2H, J = 6.9 Hz, CH_2). ^{13}C NMR (75 MHz, $CDCl_3$) (δ, ppm): 149.59, 145.92, 137.52, 134.47, 133.91, 129.11, 128.77, 128.14, 122.84, 120.54, 115.72, 114.28, 112.34, 111.14, 63.56, 55.82, 54.22, 39.82. LC-MS (*m*/*z*):336.3 $[M+H]^+$, 693.4 [2M + Na]$^+$.

*4.1.3.8. 4-((1-Benzyl-1H-1,2,3-triazol-4-yl)methoxy)-3-methoxybenzaldehyde (**3h**).* Off white solid, M.pt. 79–81 °C, yield: 83%,R_f (Ethyl acetate/Pet. ether, 30:70) = 0.18, Anal ($C_{18}H_{17}N_3O_3$) calc. C 66.86 H 5.30 N 13.00, found: C 66.85 H 5.27 N 12.96%. IR (neat): ν (cm^{-1})3150, 2959, 2937, 2857, 1678, 1585, 1508, 1460, 1425, 1397, 1341, 1261, 1160, 1136, 1030, 994, 855, 810, 784, 758, 720, 700. ^{1}H NMR (300 MHz, $CDCl_3$) (δ, ppm): 9.86 (s, 1H, C*H*O), 7.59 (s, 1H, triazole ring), 7.46–7.37 (m, 5H, Ar–*H*), 7.29–7.22 (m, 3H, Ar–*H*), 5.54 (s, 2H, OCH_2), 5.37 (s, 2H, CH_2), 3.91 (s, 3H, OCH_3). ^{13}C NMR (75 MHz, $CDCl_3$) (δ, ppm): 190.90, 153.03, 149.95, 143.62, 134.27, 130.64, 129.17, 128.89, 128.18, 126.68, 123.10, 112.69, 109.27, 62.98, 55.99, 54.32. LC-MS (*m*/*z*):324.3 $[M+H]^+$, 669.3 [2 M + Na]$^+$.

4.2. X-ray crystallographic analysis

The structure of the compound **3d** was unequivocally established by X-ray crystallographic analysis. Single crystal of **3d** was obtained through the slow evaporation of its ethanol solution. A suitable crystal ($C_{17}H_{17}N_3O_2$, compound **3d**) was selected and analysed on a Nonius Kappa CCD APEXII diffractometer equipped with rotating anode generator, the radiation was monochromated with a Montel mirror (Mo Kα = 0.71073 Å). Intensity data were collected at 223K using ϕ and ω scans. No significant loss in intensities was observed during data collection. Multi-scan absorption corrections were applied to the intensity data empirically using Denzo [17]. Data collection, reduction, and refinement were performed using Collect [18] and Denzo-SMN [19] software. Crystal structure was solved by direct methods using SHELXS-97 [20] and refined with full-matrix least-squares based on F^2 using SHELXL-97 [20]. All non-hydrogen atoms were refined anisotropically. Hydrogens were first located in the Fourier difference map, then positioned geometrically and allowed to ride on their respective parent atoms. The molecular graphics and crystallographic illustrations were prepared using PLATON [21] and MERCURY [22].

4.3. In vitro anticandidal activity

A broth dilution technique was employed to determine the IC_{50} value for all the synthesized 1,2,3 triazole derivatives (**3a-3h**) and their precursor molecules (**1a-h**) against three strains of *Candida*. The test compounds were dissolved in DMSO with less than 4% concentration of DMSO in the final test volume. Various concentrations (1000 … 7.8 μg/mL) of test compounds were dispensed into wells, then inoculated with test organism with approx. 2.5×10^3 cells/mL and incubated at 37 °C for 24 h. After incubation period, the optical density was measured at 600 nm by using Thermo Scientific Multiskan Go plate reader. The IC_{50} value was defined as the concentration of the test compound that causes 50% decrease in absorbance compared with that of the control (no test compound). The MFC values were determined as the lowest concentration resulting in no growth on the subculture of 100 μL aliquot from wells without turbidity on YEPD agar after 48 h of incubation period at 37 °C for *Candida* cells [23]. All the experiments were done in triplicate in separate time.

4.4. FIC index

The fractional inhibitory concentration (FIC) index is defined as the sum of the MIC of each drug when used in combination divided

by the MIC of the drug used alone. Synergy and antagonism were defined by FIC indices of ≤0.5 and >4, respectively. An FIC index result of >0.5 but ≤4 was considered indifferent [24]. Both, compound **3e** and FLC were serially diluted in growth medium upto the concentration of 0.48 μg/mL and 0.24 μg/mL, respectively. The MIC values of compound alone and in combination with FLC were determined by broth micro dilution method in 96 well plate.

4.5. Cytotoxicity assays

4.5.1. Hemolysis

The hemolytic activities of the test compounds **1e**, **1h**, **3e**, **3h** and fluconazole were determined on human red blood cells [25]. Human blood from healthy individual was collected in tubes containing EDTA as anti-coagulant. The erythrocytes were harvested by centrifugation for 10 m at 2000 rpm and 20 °C, washed three times in PBS. To the pellet, PBS was added to yield a 10% (v/v) erythrocytes/PBS suspension. The 10% suspension was then diluted 1:10 in PBS. From each suspension, 100 μL was added in triplicate to 100 μL of a different dilution series of test compounds in the same buffer in Eppendorf tubes. Total hemolysis was achieved with 1% Triton X-100. The tubes were incubated for 1 h at 37 °C and then centrifuged for 10 min at 2000 rpm and 20 °C. From the supernatant fluid, 150 μL was transferred to a flat-bottomed microtiter plate (Tarson), and the absorbance was measured spectrophotometrically at 450 nm. The hemolysis percentage was calculated by following equation:

$$\%\text{Hemolysis} = [(A_{450}\text{ of test compound treated sample} - A_{450}\text{ of buffer treated sample})/(A_{450}\text{ of 1\% Triton X} - 100\text{ treated sample} - A_{450}\text{ of buffer treated sample})] \times 100\%.$$

4.5.2. Cytotoxicity by cell proliferation assay

The *in vitro* cytotoxicity of compounds (**3a-h**) to mammalian cells was also determined. The assay was performed in 96-well tissue culture-treated plates as described earlier [26]. Vero cells (monkey kidney fibroblasts) were seeded to the wells of 96-well plate at a density of 25,000 cells/well and incubated for 24 h. Samples at different concentrations were added and plates were again incubated for 48 h. The number of viable cells was determined by Neutral Red assay. IC_{50} values were obtained from dose response curves. Doxorubicin was used as a positive control for cytotoxicity.

4.6. QSAR analysis

The activity data i.e. IC50 were converted into the logarithmic scale pIC50 (pIC50 = -logIC50) and then proceed the QSAR analysis as the response variables. The data set was divided into the two subsets. (Training and test set). Training set contained 12 compounds and test set had 4 compounds. The test set compounds were selected manually considering the distribution of biological data and structural diversity. The training set was used to build a regression model, and the test set was used to evaluate the predictive ability of the model obtained.

All the molecular structures have optimized using the density functional method B3LYP/6-31G** using Gaussian03 [27]. Molecular descriptors were calculated using CODESSA [28]. A total of 163 molecular descriptors were calculated, including constitutional, topological, electro statistic, geometrical, Quantum chemical, 1D and 2D, functional groups atom centered fragments, etc. Heuristic method has been used to generate the QSAR model and the measurement of statistical parameters.

Acknowledgement

Mohammad Abid gratefully acknowledges the funding support in the form of Young Scientist from Science & Engineering Research Board (Grant No. SR/FT/LS-03/2011), New Delhi, INDIA and University Grant Commission (UGC), Govt. of India (Grant No. 41–277/2012 (SR)). MI and BA would like to acknowledge UGC, INDIA for non-NET fellowship.

Appendix A. Supplementary data

Supplementary data related to this article can be found at http://dx.doi.org/10.1016/j.ejmech.2015.02.007.

Conflict of interest

No conflict of interest.

References

[1] CDC, U.S. Department of Health and Human Services, Atlanta, Georgia, 2013, pp. 63–64.
[2] M.A. Hossain, M.A. Ghannoum, Exp. Opin. Invest. Drugs 9 (2000) 1797–1813.
[3] M. Matsuoka, T. Kitao, J. Heterocycl. Chem. 29 (1992) 439–442.
[4] Y.B. Kim, S.K. Kim, Bioorg. Med. Chem. Lett. 14 (2004) 541–544.
[5] L. Gavara, P. Moreau, Eur. J. Med. Chem. 45 (2010) 5520–5526.
[6] A. Passannanti, G. Cirrincione, Heterocycles 48 (1998) 1229–1235.
[7] M.D. Chen, S.Y. Yang, X.L. Du, Heterocycl. Comm. 6 (2000) 421–426.
[8] E.A. Sherement, V. Berestovitsk, Russ. J. Org. Chem. 40 (2004) 594–595.
[9] B.S. Holla, N.S. Kumari, Eur. J. Med. Chem. 40 (2005) 1173–1178.
[10] A.C. Cunha, E.J. Barreiroa, Bioorg. Med. Chem. Lett. 11 (2003) 2051–2059.
[11] M. Abid, S.M. Agarwal, A. Azam, Eur. J. Med. Chem. 43 (9) (2008) 2035–2039.
[12] M. Abid, A.R. Bhat, F. Athar, A. Azam, Eur. J. Med. Chem. 44 (1) (2009) 417–425.
[13] C.K. Johnson, ORTEP, Report ORNL 3794, Oak Ridge National Laboratory, Tennessee, USA, 1965.
[14] A.R. Kelly, J. Wei, S. Kesavan, J.C. Marie, N. Windmon, D.W. Young, L.A. Marcaurelle, Org. Lett. 11 (11) (2009) 2257–2260.
[15] J.H. Lee, S. Gupta, W. Jeong, Y.H. Rhee, J. Park, Angew. Chem. Int. Ed. 51 (2012) 10851–10855.
[16] S.P. Chakrabarty, R. Ramapanicker, R. Mishra, S. Chandrasekaran, H. Balaram, Bioorg. Med. Chem. 17 (2009) 8060–8072.
[17] Z. Otwinowski, D. Borek, W. Majewski, W. Minor, Acta Cryst. A59 (2003) 228.
[18] Z. Otwinowski, W. Minor, Methods Enzymol. 276 (1997) 307.
[19] COLLECT, Data Collection Software, Nonius BV, Delft, 1998.
[20] G.M. Sheldrick, Acta Cryst. 64A (2008) 112.
[21] A.L. Spek, J. Appl. Cryst. 36 (2003) 7–13.
[22] C.F. Macrae, I.J. Bruno, J.A. Chisholm, P.R. Edgington, P. McCabe, E. Pidcock, L. Rodriguez-Monge, R. Taylor, J. van de Streek, P.A. Wood, J. Appl. Cryst. 41 (2008) 466–470.
[23] NCCLS, Reference Method for Broth Dilution Antifungal Susceptibility Testing of Yeasts; Approved Standard M27–A2, National Committee on Clinical Laboratory Standards, Wayne, P.a., 2002, pp. 8–9, 22.
[24] F.C. Odds, A.J. Brown, N.A. Gow, Trends Micribiol. 11 (2003) 272–279.
[25] A. Khan, A. Ahmad, I. Xess, L.A. Khan, N. Manzoor, Phytomedicine 17 (2010) 921–925.
[26] S. Manohar, U.C. Rajesh, S.I. Khan, B.L. Tekwani, D.S. Rawat, ACS Med. Chem. Lett. 3 (2012) 555–559.
[27] M.J. Frisch, G.W. Trucks, H.B. Schlegel, G.E. Scuseria, M.A. Robb, J.R. Cheeseman, J.A. Montgomery, J.T. Vreven, K.N. Kudin, J.C. Burant, J.M. Millam, S.S. Iyengar, J. Tomasi, V. Barone, B. Mennucci, M. Cossi, G. Scalmani, N. Rega, G.A. Petersson, H. Nakatsuji, M. Hada, M. Ehara, K. Toyota, R. Fukuda, J. Hasegawa, M. Ishida, T. Nakajima, Y. Honda, O. Kitao, H. Nakai, M. Klene, X. Li, J.E. Knox, H.P. Hratchian, J.B. Cross, C. Adamo, J. Jaramillo, R. Gomperts, R.E. Stratmann, O. Yazyev, A.J. Austin, R. Cammi, C. Pomelli, J.W. Ochterski, P.Y. Ayala, K. Morokuma, G.A. Voth, P. Salvador, J.J. Dannenberg, V.G. Zakrzewski, S. Dapprich, A.D. Daniel, M.C. Strain, O. Farkas, D.K. Malick, A.D. Rabuck, K. Raghavachari, J.B. Foresman, J.V. Ortiz, Q. Cui, A.G. Baboul, S. Clifford, J. Cioslowski, B.B. Stefanov, G. Liu, A. Liashenko, P. Piskorz, I. Komaromi, R.L. Martin, D.J. Fox, T. Keith, M.A. Al-Laham, C.Y. Peng, A. Nanayakkara, M. Challacombe, P.M.W. Gill, B. Johnson, W. Chen, M.W. Wong, C. Gonzalez, J.A. Pople, GAUSSIAN 03, Revision B.04, Gaussian, Inc., Pittsburgh, 2003.
[28] T.M. Codessa, V.2.7.10 (PC), Semichem, 7204 Mullen, Copyright Semichem and the University of Florida, Shawnee, KS, USA, 2002.